Environmental Science & Technology

Article

pubs.acs.org/est

Indoor Ultrafine Particles of Outdoor Origin: Importance of Window Opening Area and Fan Operation Condition

Donghyun Rim,* Lance A. Wallace, and Andrew K. Persily

National Institute of Standards and Technology, 100 Bureau Drive, MS8633 Gaithersburg, Maryland 20899, United States

Supporting Information

ABSTRACT: Inhalation exposure to ambient ultrafine particles (UFP) has been shown to induce adverse health effects such as respiratory and cardiovascular mortality. Human exposure to particles of outdoor origin often occurs indoors due to entry of UFP into buildings. The objective of the present study is to investigate entry of UFP into a building considering building operational characteristics and their size-dependent effects on UFP concentrations. Indoor and outdoor UFP concentrations along with air change rates were continuously measured in a full-scale test building. Estimates of infiltration factor, penetration coefficient, and deposition rate have been made for a range of particle sizes from 4 to 100 nm. The results show that UFP infiltration factor varies with particle diameter, window position, air change rate, and central fan operation. When the central fan was on continuously, the average infiltration factor ranged from 0.26 (particles <10 nm) to 0.82 (particles >90 nm) for two large window openings, and from 0.07 to 0.60 for two small window openings. Under the central fan-off condition, the average infiltration factor ranged from 0.25 (particles <10 nm) to 0.72 (particles >90 nm) for two small window openings, while it ranged from 0.01 to 0.48 with all windows closed. Larger window openings led to higher infiltration factors due to the larger extent of particle penetration into the building. The fan operation mode (on vs off) also has a strong impact, as the infiltration factor was consistently lower (up to 40%) when the fan was on due to additional particle deposition loss to the furnace filter and duct surfaces.

INTRODUCTION

Ultrafine particles (UFP, <100 nm in diameter) have been associated with adverse health effects such as oxidative damage to DNA[1] and mortality.[2] Their small size allows them to penetrate cells, where they induce inflammation in the respiratory tract that potentially leads to asthma and other respiratory impairments.[3,4] UFP can enter the bloodstream, damaging sites in the cardiovascular system.[5] Their large surface-to-volume ratio may result in their toxic components being more biologically available than those of larger particles.[3,6] Human exposure to airborne ultrafine particles (UFP) mainly occurs indoors, where people spend about 90% of their time.[7] Indoor UFP concentrations are affected both by indoor sources and by entry of UFP from outdoors. Sources of urban outdoor UFP are mainly combustion products from gasoline and diesel engines,[8] and "nucleation bursts" from natural atmospheric reactions.[9] Indoor UFP sources include consumer products;[10,11] combustion due to gas stoves, gas clothes dryers, cigarettes, and candles;[12−15] heating elements in electric stoves, hair dryers, steam irons, and other personal appliances;[14,16] and electric motors in common household appliances.[17]

In the absence of indoor sources, the UFP concentrations in buildings are governed by the entry of outdoor air particles via infiltration and ventilation (both natural and mechanical). The infiltration factor (F_{inf}) relates equilibrium indoor concentrations to outdoor concentrations in the absence of indoor sources. F_{inf} is a dimensionless quantity defined as the equilibrium fraction of outdoor UFP that penetrates indoors and remains airborne. Accordingly, high values of F_{inf} result in elevated levels of inhalation exposure to UFP of outdoor origin. There are three main variables that influence F_{inf}: particle penetration efficiency (P), deposition loss rate (k), and air change rate (a). These parameters (F_{inf}, P, a, and k) vary among buildings depending on building characteristics and outdoor conditions. Several studies[18−22] have monitored continuous indoor and outdoor UFP concentrations in multiple homes under uncontrolled conditions. However, there have been relatively few controlled studies of the effects of building environmental and operating conditions on variability of F_{inf}, P, and k for UFP. Only a few studies[23−25] have provided controlled effects of building conditions (i.e., opening windows) on general trend of F_{inf}, P, and k for UFP. Rim et al.[24] provided indoor−outdoor UFP dynamics for all windows closed and one window open conditions. The present study

Received: September 6, 2012
Revised: January 15, 2013
Accepted: January 23, 2013
Published: February 5, 2013

Table 1. Experiment Conditions

test ID	date	total window opening area (cm^2)	central fan mode (on/off)	avg air change rate (SD) (h^{-1})	avg indoor temp (SD) (°C)	avg outdoor temp (SD) (°C)
LWOn1	10/1−10/4/10	2600	on	0.99 ± 0.39	20.9 ± 1.7	13.3 ± 3.4
LWOn2	10/8−10/12/10	2600	on	0.83 ± 0.28	26.2 ± 2.2	18.1 ± 5.2
LWOn3	10/15−10/18/10	2600	on	1.23 ± 0.66	19.5 ± 2.3	11.3 ± 6.8
LWOn4	10/22−10/25/10	2600	on	0.90 ± 0.30	21.8 ± 2.8	12.8 ± 6.0
LWOn5	11/12−11/15/10	2600	on	0.74 ± 0.37	18.5 ± 2.4	8.3 ± 5.3
LWOn6	11/26−11/29/10	2600	on	1.41 ± 0.70	15.7 ± 1.0	2.0 ± 3.0
SWOn1	7/8−7/11/11	1300	on	0.86 ± 0.40	24.7 ± 0.51	24.6 ± 4.1
SWOn2	7/14−7/17/11	1300	on	0.85 ± 0.40	24.0 ± 0.5	26.0 ± 4.8
SWOn3	8/5−8/8/11	1300	on	1.04 ± 0.48	24.3 ± 0.53	23.0 ± 4.2
SWOn4	8/19−8/22/11	1300	on	0.89 ± 0.36	24.7 ± 0.47	26.4 ± 3.4
SWOn5	9/9−9/12/11	1300	on	1.00 ± 0.47	22.0 ± 0.71	22.9 ± 4.3
SWOn6	9/2−9/6/11	1300	on	0.76 ± 0.35	21.8 ± 0.50	21.6 ± 3.9
CWOff1	1/20−1/24/11	0	off	0.20 ± 0.03	12.5 ± 2.1	0.4 ± 3.3
CWOff2	1/27−2/1/12	0	off	0.21 ± 0.04	14.5 ± 2.4	6.0 ± 4.8
CWOff3	2/3−2/6/12	0	off	0.18 ± 0.02	12.9 ± 1.6	−0.95 ± 2.9
CWOff4	5/17−5/20/12	0	off	0.19 ± 0.04	25.2 ± 2.9	19.1 ± 5.9
CWOff5	5/22−5/25/12	0	off	0.16 ± 0.05	28.6 ± 1.2	22.4 ± 3.3
CWOff6	5/30−6/2/12	0	off	0.21 ± 0.05	25.9 ± 1.5	20.1 ± 4.1
SWOff1	11/4−11/7/11	1300	off	1.23 ± 0.55	16.0 ± 2.1	6.2 ± 4.7
SWOff2	12/2−12/5/11	1300	off	1.54 ± 0.61	13.7 ± 1.7	6.3 ± 4.3
SWOff3	12/9−12/13/11	1300	off	1.08 ± 0.27	13.5 ± 1.3	0.87 ± 3.9
SWOff4	6/25−6/27/12	1300	off	0.80 ± 0.33	25.2 ± 1.8	21.1 ± 5.0

expands on the study by Rim et al.,[24] in particular by considering building operational characteristics and UFP size-dependent effects on indoor concentrations. The study aims to investigate F_{inf}, P, and k for size-resolved UFP ranging from 4 to 100 nm as a function of central air distribution fan operation and window opening area.

METHODS

Test House. Experimental measurements were conducted in a full-scale test house located in Gaithersburg, MD (Figure S1, Supporting Information (SI)).[26] It consists of three bedrooms, two baths, kitchen, and a family, dining, and living area. The house has a floor area of 140 m^2 and a volume of 340 m^3. In the test house, indoor and outdoor monitoring of UFP concentrations was conducted during weekends between October 2010 and July 2012. Since the test house was sometimes in use for other experiments and possibly had indoor sources at those times, only weekends when the house was uninhabited were selected for the experimental periods. Excluding the monitoring periods influenced by calibration, maintenance, and troubleshooting of the instruments, a total of 22-weekend measurements (Table 1) were considered for subsequent analysis. Throughout this paper, all tests are referred to with unique test identifiers, shown in the first column of Table 1, where the first set of characters (LW/SW/CW) represents window opening area, the next set of characters determines the central fan operating mode (On/Off), and the last represents the repetition number of the test. LW represents large window opening area (two windows open with 1300 cm^2 each), SW indicates small window opening area (two windows open with 650 cm^2 each), and CW is closed windows. Table 1 summarizes sampling time, building operating conditions, and indoor and outdoor environmental conditions for each test.

Experiment Conditions. As shown in Table 1, the measurements were conducted under different operation modes of the central air recirculation fan and window opening area. For each weekend measurement, the indoor and outdoor UFP concentrations (4−100 nm) were monitored for three consecutive days. Six tests were conducted with the large window opening area (LW), ten with the small window opening area (SW), and six with closed windows (CW). The central fan operating mode was tested against only two window opening conditions: SW and CW. Although the correlation between local meteorology and UFP infiltration factor was not analyzed, Table S1 in the SI provides wind data collected from the weather station approximately 1 km away from the test building. The weather data were available until October 2011, after which the weather station was not operating properly.

Experimental Monitoring. Size-resolved UFP measurements were made using a scanning mobility particle sizer (SMPS, 3936N88, TSI Inc., Shoreview, MN) that consists of a nano-differential mobility analyzer (nano-DMA), electrostatic classifier, and a water-based condensation particle counter (WCPC). The system was operated at a flow setting of 0.6 L/min sampling flow (sheath flows of 6 L/min). Flow rates were measured in triplicate before each experiment began and were required to be within a 3% range. This setting allowed a particle size range from 3 to 100 nm. This size range included about 97 equidistant size categories (on a logarithmic scale). The full range was sampled on a 2.5-min cycle, including 2 min of sampling followed by 30 s during which the voltage was lowered to prepare for the next scan. An automatic switching unit was built to allow the SMPS to sample outdoor and indoor air alternately. Four outdoor scans (10 min total) were followed by four indoor scans and so on. The first scan in each new microenvironment was compared to the following three scans to determine a possible effect of the change in micro-environmental conditions (temperature, relative humidity, atmospheric pressure) on the instrument readings. If the first scan was considerably different from the following 3 scans, it was dropped or replaced by the average of the other three

scans; however, this happened rarely (<5% of the time). Each measurement event typically provided about 60−72 consecutive hours of sampling with about 1400−1700 scans.

To measure time-varying air change rate in the house, injections of the tracer gas (sulfur hexafluoride, SF_6) were made in the living room at 4- or 2-h intervals by an automated system, which allowed all measurements to be made when the test house was uninhabited. The decay in tracer gas concentrations was monitored at 10-min intervals at seven locations in the house (three bedrooms, living room, family room, dining room, and kitchen). The concentrations were measured using gas chromatography with electron capture detection (GC/ECD), and the air change rate was calculated for each of the seven rooms by regressing the logarithm of the SF_6 concentration against time over a 70-min period. When the central mechanical fan was on, supply air flowed through the ventilation system at the rate of 2000 m^3/h, or nearly 6 house volumes per hour. However, the system operated under full recirculation with no outdoor air intake. In the case of the central fan on, tracer gas concentrations were typically similar across all rooms of the house with <5% relative standard deviation (RSD) within 10 min of injection. Under closed-window conditions, the air change rates typically agreed across all rooms to within 10% RSD. When one or two windows were open, the majority of RSDs remained within 10%; however, the rooms with the open windows sometimes had different tracer gas decay rates leading to increased RSDs, but still generally within 20% of the average rate. In the case with the central fan off, RSDs were generally within 20% of the average rate for the case of SW (small window opening area); however, the majority of RSDs were higher than 20% for the LW (large window opening area) case therefore the tests with LW and the central fan off were excluded from the present study. These higher RSDs with the central fan off are primarily due to poor mixing, associated with the rooms with the open windows having high air change rates and the other rooms having low rates. Note that the 3-day average air change rate observed in this study ranged from 0.74 to 1.41 h^{-1} for LW condition, 0.76 to 1.54 h^{-1} for SW condition, and 0.16 to 0.21 h^{-1} for CW condition. These values are comparable to those seen in a previous study by Rim et al.[24] that measured air change rates ranging from 0.14 to 0.44 h^{-1} for CW condition and 0.18 to 0.63 h^{-1} for one window open (650 cm^2).

Quality Control and Measurement Uncertainty. For quality assurance purposes, the tracer gas analyzer was calibrated every week against known concentrations ranging from 20 to 1200 $\mu g/m^3$ (18 point calibration) with the limit of detection of 6 $\mu g/m^3$. The calibration parameters of the monitoring instrument (GC/ECD) sometimes drifted between successive calibrations. Therefore, the error due to drift of the instrument was analyzed by observing the variation of calibration slope and intercept for successive calibrations. In addition, the measurement errors due to incomplete mixing between rooms and the precision (repeatability of the measurement of the same concentration) were analyzed. Most of the errors associated with the calibration drift and incomplete air mixing in the house were less than 8%, and the maximum error was 13% (for large window opening condition). The errors in estimating the slope of the regression for air change rates were between 2% and 16%, with most of those being <10%. Therefore, by adding the error associated with the regression slope in quadrature with the mixing/calibration error, the average error for air change rate estimates was around 10% with a maximum error of about 20%. The uncertainty of the SMPS in measuring UFP number concentration is estimated to be 12% based on combining the individual uncertainties due to airflow rate, particle charge distribution, voltage adjustment, and particle charge efficiency in quadrature.[27] Indoor and outdoor UFP samples were collected at a height of 1.5 m above the floor and ground. Particle deposition occurred in the sampling tubes and the particle losses in the sampling tubes were measured. The lengths of the indoor and outdoor sampling tubes were roughly the same (≈ 50 cm), and even though the indoor sampling tube had a bend of approximately 130 degrees, the difference in particle loss between sampling the two tubes was estimated to be less than 7%.

Estimation of Infiltration Factor, Penetration Efficiency, and Deposition Rate. Indoor concentration of outdoor UFP depends on the ability of the particles to penetrate the building envelope and their subsequent deposition rate onto indoor surfaces. In the present study, entry of UFP into a building was estimated for the cases of central fan on and off along with three window opening positions: closed-window, two windows open 7.5 cm (window opening area of 650 cm^2 for each window), and two windows open 15 cm (window opening area of 1300 cm^2 for each window). In the absence of indoor sources, the indoor concentration (C_{in}) resulting from the entry of outdoor particles can be expressed by the mass balance equation

$$\frac{dC_{in}}{dt} = PaC_{out} - (a + k)C_{in} \quad (1)$$

where P is the penetration coefficient (dimensionless); a is the air change rate (h^{-1}); k is the deposition rate (h^{-1}), and C_{in} and C_{out} are the indoor and outdoor UFP number concentrations, respectively (no./cm^3). Note that this and subsequent equations apply to each of the 97 size bins monitored by the SMPS. The values of P and k are a function of the size bin.

The equilibrium solution ($(dC_{in})/(dt) = 0$) for each particle size category is given by

$$C_{in} = \frac{Pa}{a + k}C_{out} \quad (2)$$

where the fraction of outdoor air particles found indoors at equilibrium is the infiltration factor F_{inf}:

$$F_{\mathrm{inf}} = \frac{Pa}{a + k} \quad (3)$$

F_{inf} varies among homes and is a function of the penetration coefficient (P) and deposition rate (k). The penetration coefficient (P) represents the fraction of outdoor air particles that pass through building cracks, leakage paths, and window openings, while deposition rate (k) is the rate of particle deposition loss onto interior surfaces, including ductwork and furnace filters. It is difficult to measure P and k directly and there are few data in the literature on the levels or variability of P and k for size-resolved UFP within buildings, particularly in relation to building operating conditions. The experiments in conjunction with analytical modeling performed in the present study reveal how building conditions such as opening windows and operating the central furnace fan affect penetration and deposition characteristics of UFP.

In the test house, experiments monitored three time-varying variables: air change rate (a), indoor concentration (C_{in}), and outdoor concentration (C_{out}). The difference form of the mass

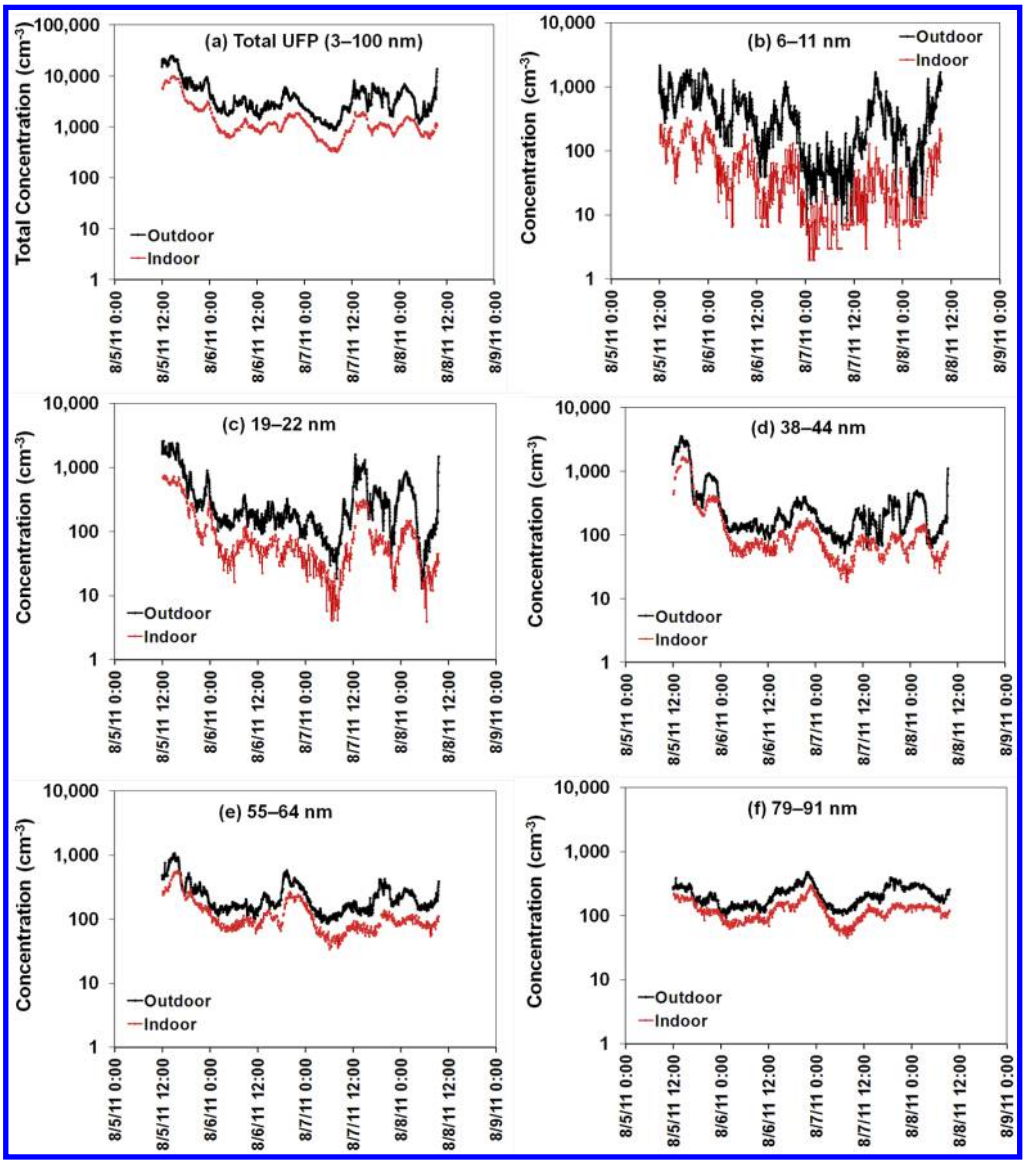

Figure 1. Indoor and outdoor number concentrations for different sizes of UFP over the test period (SWOn3, Aug 5–8, 2011): (a) total UFP (3–100 nm); (b) 6–11 nm; (c) 19–22 nm; (d) 38–44 nm; (e) 55–64 nm; (e) 79–91 nm.

balance model, a so-called recursive model, was used to estimate F_{inf}, P, and k Details of the analytical approach to estimating values of P, k, and F_{inf} are described in the SI.

The calculated infiltration factor (F_{inf}) was also validated by comparing it to the ratio of average indoor and outdoor concentration (I/O ratio) as follows, given that F_{inf} is expected to be equal to the time-averaged I/O ratio in the absence of indoor sources (see eq 2).

$$\text{I/O ratio} = \frac{C_{in.Avg}}{C_{out.Avg}} \quad (4)$$

Since the indoor concentration lags the outdoor level, the I/O ratio at any time may be far from equilibrium. However, as the outdoor concentration fluctuates, the indoor concentration will be alternately above and below the equilibrium concentration, and therefore as the averaging time increases, the I/O ratio likely approaches the equilibrium value.

RESULTS AND DISCUSSION

Indoor–Outdoor Concentrations. Time series plots of indoor and outdoor UFP measurements were generated for each weekend test. Figure 1 presents examples of temporal variation of number concentrations for total UFP (a) and five particle size categories (b–f) during test SWOn2. Daily variations were found, with both indoor and outdoor concentrations generally higher during the day, perhaps due to increased traffic volume and atmospheric photochemical reactions. Since there were no indoor activities that could elevate indoor UFP levels, the indoor concentrations were generally lower than outdoor concentrations. The temporal change in the indoor concentration was caused by fluctuations in outdoor particle number and by changes in the outdoor air change rate.

Model Analysis Results. Figure S2 in the SI illustrates an example of the recursive model analysis used to predict time-varying indoor concentrations and the regression analysis between the measured and modeled indoor concentration. For this specific case (for profiles for particle size ranging from 19

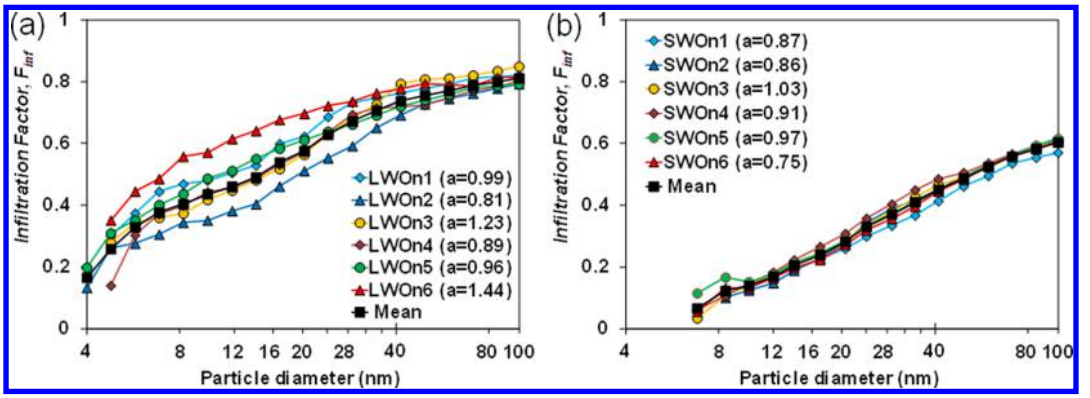

Figure 2. Size-dependent infiltration factor: (a) large window opening (LW); (b) small window opening (SW). The central mechanical fan was operating continuously.

to 22 nm for the test SWOn3), the penetration coefficient P and deposition rate k that predicted the measured (time-varying) concentrations with the least sum of squared error were 0.50 and 0.74 h^{-1}, respectively. The R^2 value for the regression was 0.98 and the resulting infiltration factor F_{inf} based on eq 3 was 0.29. Individual estimates of uncertainty for P and k based on the relative standard deviations for the least sum square approach[28] are 0.5% and 1.9%, respectively. All individual errors in estimating P and k for selected representative tests are described in SI Table S2. Note that the estimated errors are the lower bound of the actual expected uncertainties assuming perfect measurements of C_{in}, C_{out}, and a. However, adding the measurement uncertainties of each term (C_{in}, C_{out}, a) in eq 1 in quadrature shows that the actual uncertainties of P and k are mostly smaller than 20%. Therefore, considering the ranges of uncertainties in estimates of a, P, and k in eq 3, the lower and upper bound of the uncertainties of F_{inf} estimates are 13% and 35%, respectively. Table S3 in the SI presents the details of the uncertainties of F_{inf} estimates for selected representative tests and particle sizes.

Given the size dependence of the penetration and deposition parameters, Figure 2a and b show size-resolved F_{inf} calculated based on the P and k values from the recursive model and regression analysis. The recursive model predicted the indoor UFP concentration profiles with reasonable accuracy. However, due to low concentrations of ambient particles smaller than 4 nm under normal conditions and larger particle loss for smaller particle sizes, the infiltration factors were estimated only for particles >4 nm. The study results demonstrate that infiltration factor is a function of particle size and building operating conditions. The trend toward reduced infiltration factors for smaller particles is due to their increased Brownian and turbulent diffusion,[29] resulting in larger UFP losses when passing through building leakage cracks and on indoor surfaces. The F_{inf} estimate ranged from 0.13 to 0.85 for the large window opening (LW, Figure 2a) and from 0.03 to 0.62 for the small window opening (SW, Figure 2b). Comparing the two graphics (2a and 2b), F_{inf} values observed with LW are typically 0.2−0.3 higher than those with SW, suggesting that window opening area has measurable influences on the levels of indoor UPF of outdoor origin.

Given the effect of window opening on F_{inf}, Figure 3 compares size-resolved estimates of F_{inf} found in the present study and the previous study by Rim et al.[24] In the figure, the plots of F_{inf} for two windows open condition are from this study while the plots for one window open and window closed are

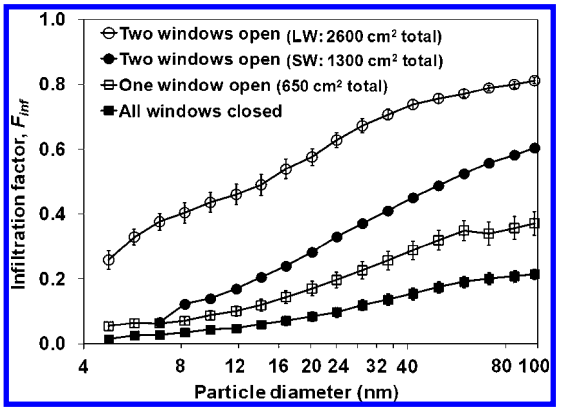

Figure 3. Infiltration factors observed for four ventilation conditions with the central mechanical fan operating in the house. The plots for the two window open condition are the results of the present study. The plots for closed window and one window open are reported in Rim et al.[24] The error bars represent the standard error of the mean of multiple tests.

from Rim et al.[24] All the data presented in Figure 3 are for the condition of the central furnace fan operating continuously.

Figure 3 shows variability and functional dependence of F_{inf} upon particle size and ventilation condition. The infiltration factor increases with window opening area, due to the combined effects of increases in air change rate and penetration. Several studies also found the dependence of F_{inf} on building ventilation conditions.[30−32] They reported that open windows lead to increase of F_{inf} for fine particles due to increased air change rate or altered particle pathway through the building.

The increase in F_{inf} with window opening area is also caused by an increase in penetration efficiency. According to eq 3, F_{inf} increases linearly with penetration efficiency. Figure 4 shows estimates of size-resolved penetration efficiency (P) for three ventilation conditions. For the closed-window case, the penetration coefficient appears to reach a plateau of about 0.5 for particles larger than about 30 nm. This behavior was also noted in a study of several inhabited apartments.[25] Since the lower penetration coefficients for smaller particles are considered to be due to increased Brownian motion, perhaps the plateau beginning around 30 nm marks the point where Brownian motion becomes unimportant for penetration through cracks. The figure demonstrates that as the window opening area increases, penetration efficiency becomes larger, presumably because more particles are entering the building through the open windows (without losses) rather than

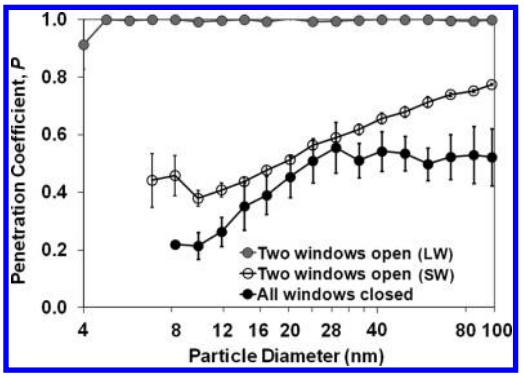

Figure 4. Penetration efficiency (P) windows closed vs two windows open (LW and SW). The plots of two windows open are the results of the present study. The plot for closed window is reported in Rim et al.[24] Error bars are standard errors of the mean of multiple tests.

through smaller leaks in the rest of the building envelope.[31] Furthermore, lower penetration efficiencies observed for smaller particles indicate more losses for smaller particles when penetrating the building envelope. This result implies that the filtering effect of building shell is more important for smaller particles; and in turn indoor sources can make more significant contribution to elevated concentrations of smaller UFP (<20 nm) than outdoor sources.

Effect of the Central Fan Operation. Besides natural ventilation through open windows, F_{inf} was influenced by the mechanical fan operating in a building. Figure 5a and b show that F_{inf} is consistently lower with the central fan operating compared to the case with the central fan off. However, the difference is more marked in the closed window case. This may be due to the low air change rate being dominated by the higher deposition rate when the fan is on. For the open window case, the air change rate is increased, and the difference in the deposition rate due to the fan being on has less effect on the infiltration factor.

Figure 6a and b compare the deposition rate (k) between the central fan off case and the central fan on case. The estimates of k are a strong function of particle size; k is largest for the smallest UFP. Depositional losses due to Brownian and turbulent diffusion of UFP that occurred on the indoor surfaces and ductwork can largely explain the higher deposition rate for the fan-on case. Along with the central fan operating, use of filters in the central mechanical system or large surface/volume ratio (e.g., many carpets, furniture, and fibrous wall surface) may also increase particle deposition loss.[33,34] The increases in particle deposition loss (k) with the use of the central mechanical fan result in smaller values of F_{inf} (eq 3).

Comparison between Infiltration Factor and I/O Ratio. There are two approaches to F_{inf} estimation: (1) the calculation based on estimates of P, k, and use of the recursive model and eq 3; and (2) the indoor/outdoor (I/O) ratio averaged over the test period assuming that there are no active indoor sources. Figure S3 compares F_{inf} and the I/O ratio of concentrations during the test SWOn3 (Aug 5–8, 2011). This figure shows that the instantaneous I/O ratio either underestimates or overestimates F_{inf} depending on whether the outdoor concentration is increasing or decreasing, due to indoor concentrations lagging outdoor levels. However, the mean values approach the equilibrium ratio over the measurement period.[18,30] In this case, the mean I/O ratio over the measurement period was 0.53 compared to the calculated F_{inf} of 0.51. In terms of average I/O ratio, uncertainty was calculated using the standard errors of the indoor and outdoor concentrations added in quadrature for eq 4. Table S3 in the SI provides details of errors and indicates that the average I/O ratios are within the range of F_{inf} .

In the present study F_{inf} estimates and average I/O ratios observed for the total of 22 weekend measurements (see SI Table S4) agree reasonably well for most of the cases, even though the discrepancy increases as the particle size decreases. Under conditions with the central fan operating, F_{inf} estimates range from 0.07 to 0.60 for small window opening (SW), and from 0.26 to 0.81 for larger window opening (LW). With the central fan off, F_{inf} estimates are between 0.25 and 0.72 for small window opening (SW) and 0.01 to 0.48 for closed windows (CW). The values of the I/O ratio found in this study are comparable to those reported in the studies in literature (see SI Table S5). Mullen et al.[19] found I/O ratios for particles (>6 nm) between 0.65 and 0.78 with windows open compared to 0.27–0.39 with window closed for three high-rise apartments in Beijing. McAuley et al.[21] reported average I/O ratios ranging from 0.12 to 0.52 (mean 0.34) for particles between 5.6 and 165 nm in diameter for five buildings in Buffalo, with the ratio being lowest (0.2) for 20 nm particles. Hahn et al.[23] measured I/O ratio for particles between 20 and 1000 nm ranging from 0.10 to 0.33 for an urban three-story unoccupied test house near a highway in Brooklyn, NY. Zhu et al.[25] showed a strong dependence of I/O ratio on particle size and ventilation mode. They reported that under natural ventilation condition with the fan off, I/O ratios of 0.6–0.9 for UFP between 70 and 100 nm

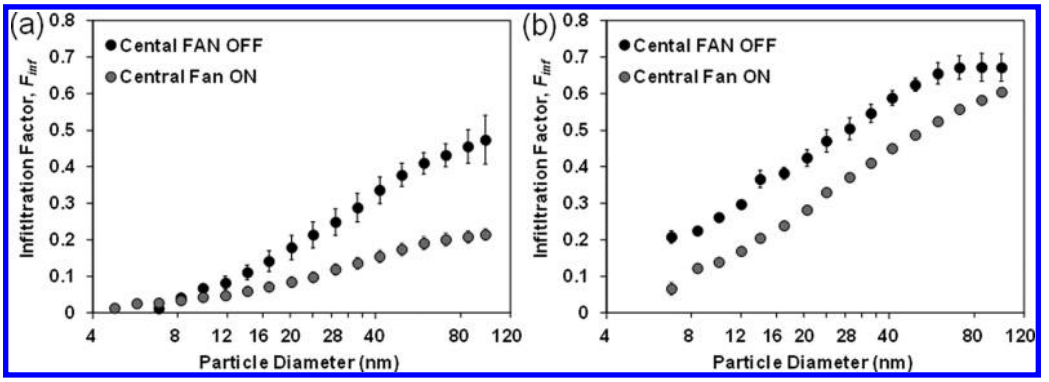

Figure 5. Size-resolved UFP infiltration factors for two modes of central fan operation (central fan on vs off): (a) all windows closed and (b) two windows open 7.5 cm each. Error bars are standard errors of the mean of multiple tests.

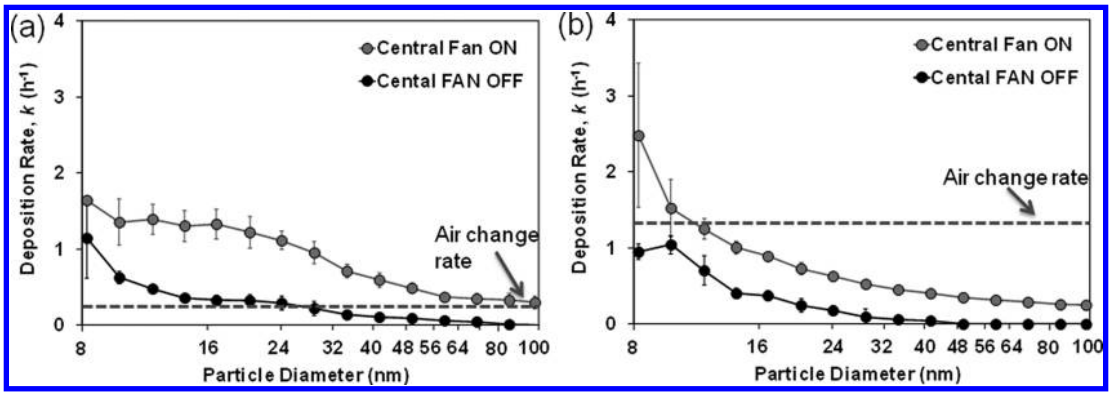

Figure 6. Size-resolved UFP deposition rates for two modes of central fan operation (central fan on vs off): (a) all windows closed and (b) two windows open 7.5 cm each. Error bars are standard errors of the mean of multiple tests.

and ratios between 0.1 and 0.4 for particles 10−20 nm. Higher ratios reported in the literature were likely due to large building leakage area, indoor sources, opening windows, or not using central mechanical fan within a building. The average I/O ratio is easier to determine than F_{inf}, given the challenges of solving nonlinear mass balance equation for quantifying F_{inf}. However, F_{inf} is quite useful for estimating personal exposure to UFP of outdoor origin in buildings,[18,22,24] while average I/O ratio data should be interpreted with caution when predicting indoor UFP concentrations of outdoor origin because of potential indoor sources that may be present during the monitoring.

Much previous work has focused on infiltration, penetration, and deposition of fine particles ($PM_{2.5}$, < 2.5 μm in diameter).[30,35−38] For most of these studies, infiltration factors ranged between 0.5 and 0.8 (see SI Table S6), with the lower values corresponding to more tightly closed homes and higher values to times when windows are more likely to be opened. The infiltration factors reported in the present study for UFP are smaller than for $PM_{2.5}$, with overall estimates of 0.01−0.48 with windows closed and 0.07−0.81 with two windows open. Kearney et al.[18] also reported that, based on their measurements (20−100 nm) in 94 homes in Windsor, Ontario, the median values of F_{inf} across homes were 0.16 (summer 2005), 0.21 (winter 2006), and 0.26 (summer 2006). This result shows that although ambient UFP is an important component of indoor UFP exposure, the influence of outdoor air UFP on indoor concentrations is relatively smaller than that for $PM_{2.5}$. Equivalently, the relative influence of indoor sources of UFP is greater than that for $PM_{2.5}$. This has implications for epidemiological studies of UFP, since monitoring of ambient UFP will provide a smaller fraction of total UFP exposure than is the case for $PM_{2.5}$.

The estimates provided here of the infiltration factor for size-resolved UFP will help establish the extent of the influence of ambient UFP on total human exposure. However, the estimates of the infiltration factor, penetration coefficient, and deposition rate presented in this study are not necessarily representative of U.S. homes or the international housing stock in general. Further studies with a larger number of buildings at regional and local scales could address the range of UFP infiltration factors across homes and the spatial variability of the infiltration factor in a specific region.

■ ASSOCIATED CONTENT

Supporting Information

Schematic diagram of the manufactured test house and detailed comparison of infiltration factor estimate (F_{inf}) and average indoor-outdoor (I/O) ratio for the total of 22 weekend measurements in the present study. This material is available free of charge via the Internet at http://pubs.acs.org.

■ AUTHOR INFORMATION

Corresponding Author

*E-mail: mcdhrim@berkeley.edu; tel: 1-512-363-8023.

Notes

The authors declare no competing financial interest.

■ ACKNOWLEDGMENTS

Participation of D.R. in this project was funded by the National Institute of Standards and Technology (NIST) through a U.S. Intergovernmental Personal Act. We thank Daniel Greb and Steven Nabinger who operated the NIST test house tracer gas analyzer and environmental systems. The full description of the procedures used in this paper requires the identification of certain commercial products and their suppliers. The inclusion of such information should in no way be construed as indicating that such products or suppliers are endorsed by NIST or are recommended by NIST or that they are necessarily the best materials, instruments, software, or suppliers for the purposes described.

■ REFERENCES

(1) Bräuner, E. V.; Forchhammer, L.; Møller, P.; Simonsen, J.; Glasius, M.; Wåhlin, P.; Raaschou-Nielsen, O.; Loft, S. Exposure to ultrafine particles from ambient air and oxidative stress-induced DNA damage. *Environ. Health Perspect.* **2007**, *115* (8), 1177−82.

(2) Stölzel, M.; Breitner, S.; Cyrys, J.; Pitz, M.; Wolke, G.; Kreyling, W.; Heinrich, J.; Wichmann, H. E.; Peters, A. Daily mortality and particulate matter in different size classes in Erfurt, Germany. *J. Expo. Sci. Environ. Epidemiol.* **2007**, *17* (5), 458−467.

(3) Oberdörster, G.; Stone, V.; Donaldson, K. Toxicology of nanoparticles: A historical perspective. *Nanotoxicology* **2007**, *1*, 2−25.

(4) Nel, A. Air pollution-related illness: Effects of particles. *Science* **2005**, *308*, 804−806.

(5) Schulz, H.; Harder, V.; Ibald-Mulli, A.; Khandoga, A.; Koenig, W.; Krombach, F.; Radykewicz, R.; Stampfl, A.; Thorand, B.; Peters, A. Cardiovascular effects of fine and ultrafine particles. *J. Aerosol Med.* **2005**, *18* (1), 1−22.

(6) Semmler-Behnke, M.; Takenaka, S.; Fertsch, S.; Wenk, A.; Seitz, J.; Mayer, P.; Oberdorster, G.; Kreyling, W. G. Efficient elimination of

inhaled nanoparticles from the alveolar region: Evidence for interstitial uptake and subsequent reentrainment onto airway epithelium. *Environ. Health Perspect.* **2007**, *115*, 728−733.
(7) Klepeis, N. E.; Nelson, W. C.; Ott, W. R.; Robinson, J. P.; Tsang, A. M.; Switzer, P.; Behar, J. V.; Hern, S. C.; Engelmann, W. H. The National Human Activity Pattern Survey (NHAPS): A resource for assessing exposure to environmental pollutants. *J. Expo. Anal. Environ. Epidemiol.* **2001**, *11*, 231−252.
(8) Kittelson, D. B. Engines and nanoparticles: A review. *J. Aerosol Sci.* **1998**, *29* (5−6), 575−588.
(9) Kulmala, M.; Vehkamäki, H.; Petäjä, T.; Dal Maso, M.; Lauri, A.; Kerminen, V.-M.; Birmili, W.; McMurry, P. H. Formation and growth rates of ultrafine atmospheric particles: A review of observations. *J. Aerosol Sci.* **2004**, *35* (2), 143−176.
(10) Colvin, V. L. The potential environmental impact of engineered nanomaterials. *Nat. Biotechnol.* **2003**, *21* (10), 1166−1170.
(11) *Performance and Accountability Report*; U.S. Consumer Product Safety Commission: Washington DC, 2011.
(12) Dennekamp, M.; Howarth, S.; Dick, C. A. J.; Cherrie, J. W.; Donaldson, K.; Seaton, A. Ultrafine particles and nitrogen oxides generated by gas and electric cooking. *Occup. Environ. Med.* **2001**, *58* (8), 511−516.
(13) Wallace, L. A.; Ott, W. Personal exposure to ultrafine particles. *J. Expo. Sci. Environ. Epidemiol.* **2011**, *21*, 20−30.
(14) Wallace, L. A.; Wang, F.; Howard-Reed, C.; Persily, A. Contribution of gas and electric stoves to residential ultrafine particle concentrations between 2 and 64 nm: Size distributions and emission and coagulation rates. *Environ. Sci. Technol.* **2008**, *42*, 8641−8647.
(15) Wallace, L. A. Ultrafine particles from a vented gas clothes dryer. *Atmos. Environ.* **2005**, *39*, 5777−5786.
(16) Schripp, T.; Kirscha, I.; Salthammera, T. Characterization of particle emission from household electrical appliances. *Sci. Total Environ.* **2011**, *409* (13), 2534−2540.
(17) Szymczak, W.; Menzel, N.; Keck, L. Emission of ultrafine copper particles by universal motors controlled by phase angle. *J. Aerosol. Sci.* **2007**, *38* (5), 520−531.
(18) Kearney, J.; Wallace, W.; MacNeill, M.; Xu, X.; VanRyswyk, K.; You, H.; Kulka, R.; Wheeler, A. J. Residential indoor and outdoor ultrafine particles in Windsor, Ontario. *Atmos. Environ.* **2011**, *45* (40), 7583−7593.
(19) Mullen, N. A.; Liu, C.; Zhang, Y.; Wang, S.; Nazaroff, W. W. Ultrafine particle concentrations and exposures in four high-rise Beijing apartments. *Atmos. Environ.* **2011**, *45* (40), 7574−7582.
(20) Wheeler, A. J.; Wallace, L. A.; Kearney, J.; Van Ryswyk, K.; You, H.; Kulka, R.; Brook, J. R.; Xu, X. Personal, indoor, and outdoor concentrations of fine and ultrafine particles using continuous monitors in multiple residences. *Aerosol Sci. Technol.* **2011**, *45* (9), 1078−1089.
(21) McAuley, T. R.; Fisher, R.; Zhou, X.; Jaques, P. A.; Ferro, A. R. Relationships of outdoor and indoor ultrafine particles at residences downwind of a major international border crossing in Buffalo, NY. *Indoor Air* **2010**, *20* (4), 298−308.
(22) Bennett, D. H.; Koutrakis, P. Determining the infiltration of outdoor particles in the indoor environment using a dynamic model. *J. Aerosol Sci.* **2006**, *37* (6), 766−785.
(23) Hahn, I.; Brixey, L. A.; Wiener, R. W.; Henkle, S. W. Parameterization of meteorological variables in the process of infiltration of outdoor ultrafine particles into a residential building. *J. Environ. Monit.* **2009**, *11*, 2192−2200.
(24) Rim, D.; Wallace, L.; Persily, A. Infiltration of outdoor ultrafine particles into a test house. *Environ. Sci. Technol.* **2010**, *44*, 5908−5913.
(25) Zhu, Y.; Hinds, W. C.; Krudysz, M.; Kuhn, T.; Fronies, J.; Sioutas, C. Penetration of freeway ultrafine particles into indoor environments. *J. Aerosol Sci.* **2005**, *36*, 303−322.
(26) Nabinger, S. J.; Persily, A. K. Impacts of airtightening retrofits on ventilation rates and energy consumption in a manufactured home. *Energy Build.* **2011**, *43* (11), 3059−3067.
(27) *Measuring Nanoparticle Size Distributions in Real-Time: Key Factors for Accuracy*; Application Note SMPS-003; TSI Incorporated: Shoreview, MN, 2007.
(28) De Levie, R. Estimating parameter precision in nonlinear least squares with Excel's Solver. *J. Chem. Educ.* **1999**, *76*, 1594−1599.
(29) Hinds, W. C. Aerosol Technology: Properties, Behavior, and Measurement of Airborne Particles, 2nd ed.; Wiley: New York, 1999.
(30) Long, C. M; Suh, H. H; Catalano, P. J; Koutrakis, P. Using time- and size-resolved particulate data to quantify indoor penetration and deposition behavior. *Environ. Sci. Technol.* **2001**, *35*, 2089−2099.
(31) Wallace, L.; Williams, A. Use of Personal-Indoor-Outdoor Sulfur Concentrations to Estimate the Infiltration Factor and Outdoor Exposure Factor for Individual Homes and Persons. *Environ. Sci. Technol.* **2005**, *39* (6), 1707−1714.
(32) Thornburg, J.; Ensor, D. S.; Rodes, C. E.; Lawless, P. A.; Sparks, L. E.; Mosley, R. B. Penetration of particles into buildings and associated physical factors. Part 1: Model development and computer simulations. *Aerosol Sci. Technol.* **2001**, *34*, 284−296.
(33) Wallace, L. A.; Emmerich, S. J.; Howard-Reed, C. Effect of central fans and in-duct filters on deposition rates of ultrafine and fine particles in an occupied townhouse. *Atmos. Environ.* **2004**, *38* (4), 405−413.
(34) Lai, A. C. K.; Nazaroff, W. W. Modeling indoor particle deposition from turbulent flow onto smooth surfaces. *J. Aerosol Sci.* **2000**, *31*, 463−476.
(35) Özkaynak, H.; Xue, J.; Spengler, J. D.; Wallace, L. A.; Pellizzari, E. D.; Jenkins, P. Personal exposure to airborne particles and metals: Results from the Particle TEAM study in Riverside, CA. *J. Exp. Anal. Environ. Epidemiol.* **1996**, *6*, 57−78.
(36) Howard-Reed, C.; Wallace, L. A.; Emmerich, S. J. Effect of ventilation systems and air filters on decay rates of particles produced by indoor sources in an occupied townhouse. *Atmos. Environ.* **2003**, *37* (38), 5295−5306.
(37) Meng, Q. Y.; Turpin, B. J.; Korn, L.; Weisel, C.; Morandi, M.; Colme, S.; Zhang, J.; Stock, T.; et al. Influence of ambient (outdoor) sources on residential indoor and personal $PM_{2.5}$ concentrations: Analyses of RIOPA data. *J. Exp. Anal. Environ. Epidemiol* **2005**, *15*, 17−28.
(38) Chen, C.; Zhao, B. Review of relationship between indoor and outdoor particles: I/O ratio, infiltration factor and penetration factor. *Atmos. Environ.* **2011**, *45*, 275−288.

Indoor ultrafine particles of outdoor origin: importance of window opening area and fan operation condition.

Supporting Information

Donghyun Rim*, Lance Wallace, Andrew Persily

National Institute of Standards and Technology
100 Bureau Drive, MS8633
Gaithersburg, MD 20899

*Donghyun Rim
100 Bureau Drive, MS8633, Bldg 226/Rm. A311
Gaithersburg, MD 20899
drim@nist.gov
301-975-4277

Number of pages: 14

Number of figures: 3

Number of tables: 6

Test House

Experimental measurements were conducted in a full-scale test house located in Gaithersburg, MD (Figure S1). It consists of three bedrooms, two baths, kitchen, and the family, dining and living area. The house has a floor area of 140 m^2 and a volume of 340 m^3. It is partially carpeted and minimally furnished. The exterior construction has fiberglass insulated 2" x 4" wood-frame walls along with exterior vinyl siding and an interior finish of vinyl covered drywall, and a vapor retarder in the walls, ceiling, and floor. The house's heating, ventilation and air-conditioning (HVAC) system consists of a 22 kW gas furnace, a 15 kW air conditioner, and a forced air recirculation fan with a design airflow rate of 470 L/s. Indoor and outdoor monitoring of UFP concentrations was conducted during weekends between October 2010 and July 2012. During the monitoring period, the house was unoccupied and indoor activities were avoided. Table S1 provides wind data (direction and speed) collected from the weather station located on the NIST campus upon the roof of a 4-story (20 m) building approximately 1 km away from the test building. The weather data was available until October 2011, after which the weather station was not operating properly.

Details of analytical approach to estimation of *P*, *k*, and $\underline{F_{inf}}$

In the test house, experiments monitored three time-varying variables: air change rate (a), indoor concentration (C_{in}) and outdoor concentrations (C_{out}). The difference form of the mass balance model (Eq. 1 in the main text) was used to estimate F_{inf}, P, and k:

$$\frac{C_{in}(i+1)-C_{in}(i)}{\Delta t} = Pa(i)C_{out}(i) - \left[a(i)+k\right]C_{in}(i) \qquad (5)$$

$$C_{in}(i+1) = Pa(i)\Delta t C_{out}(i) + \left\{1-\left[a(i)+k\right]\Delta t\right\}C_{in}(i) \qquad (6)$$

This recursive model states that the indoor concentration at time $i+1$ equals the entry of outdoor UFP via airflow into the building during the previous step plus the indoor concentration at time i minus the losses due to air change and deposition. In this model, there are three observed variables (a, C_{in} and C_{out}) and two unknown values (P, k); it is not possible to obtain two independent solutions for the two unknown values. We calculated the pair of values for P and k that minimize the sum of the absolute differences between the modeled and measured indoor concentrations. The estimated values of P and k were accepted if the R^2 of the regression of the modeled and observed indoor concentrations exceeded 80 % . The infiltration factor (F_{inf}) was then determined by calculating $Pa/(a+k)$, where a was the average air change rate over the weekend.

Figure S2 a) illustrates the recursive model analysis used to predict time-varying indoor concentrations for one size category (19 nm to 22 nm) based on the observed outdoor concentrations and air change rate. Figure S2 b) shows the regression analysis between the measured and modeled indoor concentration. For this specific case, the penetration coefficient P and deposition rate k that predicted the measured (time-varying) concentrations with the least sum of squared error were 0.50 h^{-1} and 0.74 h^{-1}, respectively. The R^2 value for the regression was 0.98 and the resulting infiltration factor F_{inf} based on Equation (3) in the main text was 0.29. Individual estimates of uncertainty for P and k based on the relative standard deviations for the least sum square approach (29) are 0.5 % and 1.9 %, respectively. These errors were propagated in quadrature to estimate the error in Finf, yielding an error of 2.6 %.

Errors in the P and k estimates obtained from the nonlinear approach were quite small (See Table S2). Note that the estimated errors are the lower bound of the actual expected uncertainties because the non-linear regression model assumes perfect measurements of indoor/outdoor concentrations and air change rate. However, based on the measurement

uncertainties of each term (C_{in}, C_{out}, a) in Eq. (6) added in quadrature, the actual uncertainties of P and k are mostly smaller than 20 %.

Comparison of infiltration factor (F_{inf}) estimate and average indoor-outdoor ratio (I/O ratio)

Table S3 provides the uncertainties of F_{inf} and I/O ratio estimates as standard error (SE) for selected representative tests and particle sizes. The uncertainties of F_{inf} were estimated considering the ranges of uncertainties in estimates of a, P and k in Eq. (3) of the main text. The lower and upper bound of the uncertainties were 13 % and 35 %, respectively. With regard to average I/O ratio, uncertainty was calculated using the standard errors of the indoor and outdoor concentrations added in quadrature for Eq. (4) in the main text. Table S4 compares average F_{inf} estimates and average I/O observed for the total of 22 weekend measurements . The two estimates agree reasonably well for most of the cases, even though the discrepancy increases as the particle size decreases.

Figure captions

Figure S1. a) Manufactured test house; b) Floor layout of the house.

Figure S2. a) Example of indoor (time-varying) concentration profiles for particle size ranging from 19 nm to 22 nm for the test SWOn3 (Aug. 5 – Aug. 8, 2011): observed vs. model-predicted; b) Scatterplot comparing model predictions to observed indoor concentrations for the test SWOn3.

Figure S3. Comparison of Cin/Cout and Finf for one particle size category (55 nm to 64 nm) observed during the test SWOn3 (Aug. 5 to Aug. 8, 2011).

Figure S1

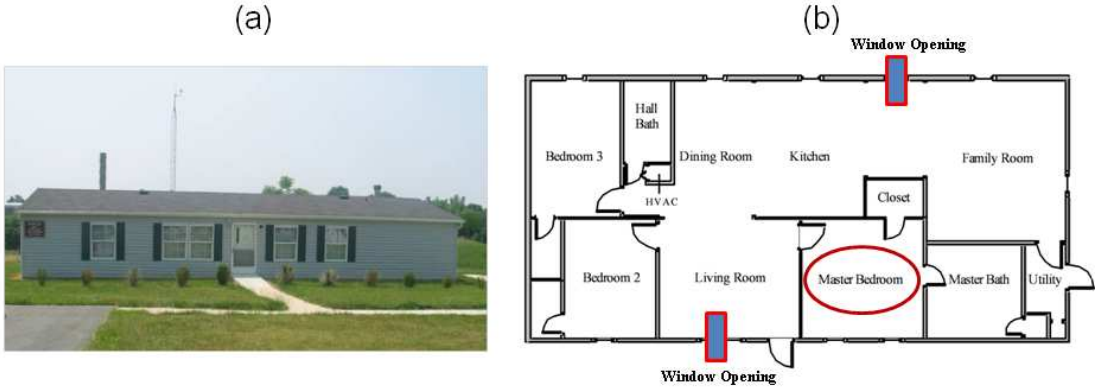

Figure S2

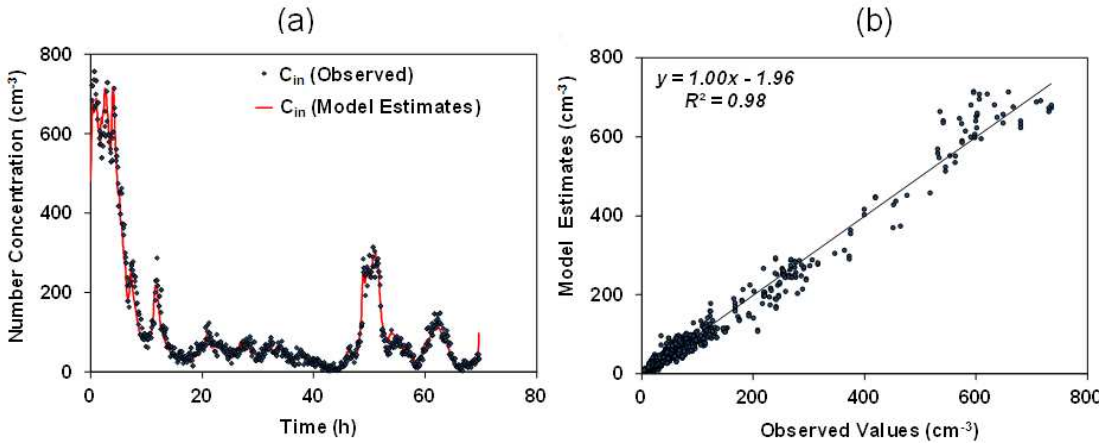

Figure S3

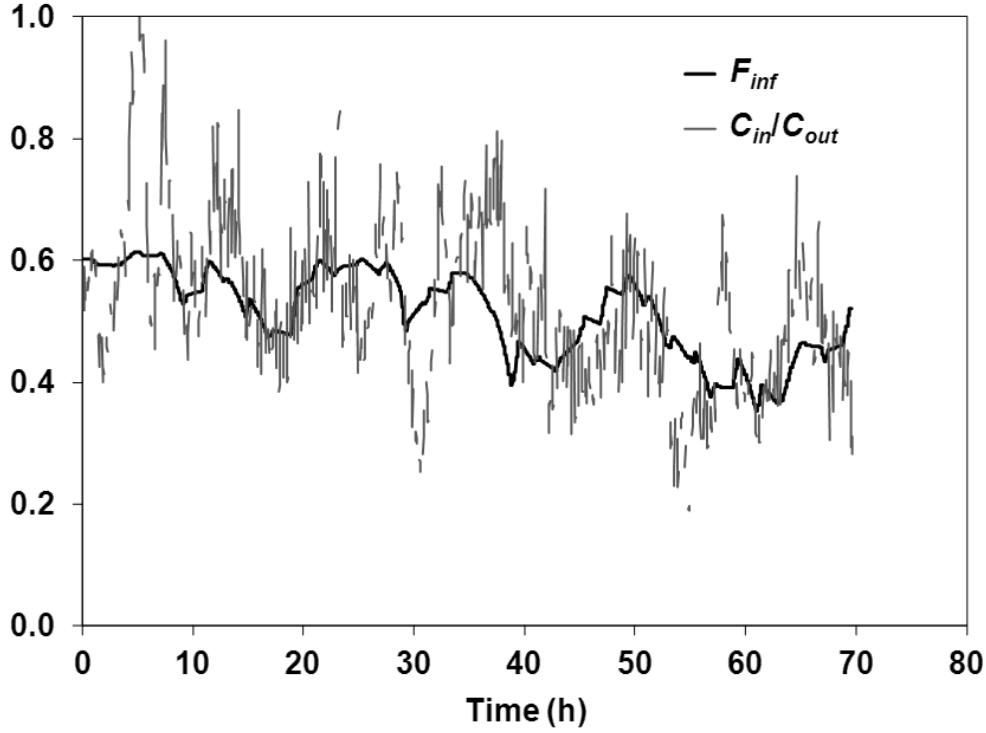

Table S1. Wind direction, wind speed, temperature difference, and relative humidity (RH)

Test ID	Date	Total Window opening area (cm^2)	Central Fan Mode (On/Off)	Wind direction (SD) (°)	Wind Speed (SD) (m/s)	Indoor Relative Humidity (%)
LWOn1	10/1-10/4/10	2600	On	206 (80)	6.3 (0.6)	48 (7)
LWOn2	10/8-10/12/10	2600	On	240 (68)	6.6 (0.9)	37 (4)
LWOn3	10/15-10/18/10	2600	On	267 (59)	7.9 (1.7)	36 (2)
LWOn4	10/22-10/25/10	2600	On	228 (51)	6.9 (1.2)	34 (5)
LWOn5	11/12-11/15/10	2600	On	182 (80)	6.2 (0.5)	29 (5)
LWOn6	11/26-11/29/10	2600	On	233 (74)	7.9 (1.0)	23 (2)
SWOn1	7/8-7/11/11	1300	On	219 (63)	6.3 (0.9)	56 (5)
SWOn2	7/14-7/17/11	1300	On	213 (46)	6.3 (1.7)	56 (6)
SWOn3	8/5-8/8/11	1300	On	216 (57)	6.6 (1.0)	51 (4)
SWOn4	8/19-8/22/11	1300	On	236 (62)	6.7 (1.1)	61 (6)
SWOn5	9/2-9/6/11	1300	On	202 (53)	6.2 (0.8)	63 (4)
SWOn6	9/9-9/12/11	1300	On	226 (77)	6.8 (0.9)	62 (6)

Table S2. Uncertainties (RSD) of *P*, *k* estimates for non-linear regression analyses.

Particle Diameter (nm)	Central Fan On				Central Fan off			
	Large Window Opening (LWOn1)		Small Window Opening (SWOn4)		Small Window Opening (SWOff4)		Closed Windows (CWOff2)	
	P (%)	*k (%)*	*P (%)*	*k (%)*	*P (%)*	*k (%)*	*P (%)*	*k (%)*
4.4 to 5.1	0.70	0.76						
5.3 to 6.2	0.82	0.43			0.43	0.65		
6.4 to 7.4	0.69	0.31	1.66	2.11	0.25	0.44		
7.6 to 8.8	0.53	0.20	0.60	0.98	0.20	0.37	1.14	1.66
9 to 11	0.50	0.16	0.27	0.62	0.16	0.30	0.63	0.96
11 to 13	0.47	0.16	0.18	0.42	0.11	0.23	0.39	0.67
13 to 15	0.41	0.21	0.14	0.35	0.09	0.22	0.29	0.55
16 to 18	0.22	0.31	0.11	0.30	0.08	0.22	0.27	0.50
19 to 22	0.14	0.28	0.10	0.29	0.08	0.26	0.28	0.51
22 to 26	0.13	0.24	0.10	0.28	0.09	0.34	0.24	0.46
27 to 31	0.17	0.25	0.09	0.26	0.08	0.35	0.26	0.54
32 to 37	0.16	0.33	0.08	0.23	0.06	0.37	0.32	0.73
38 to 44	0.14	0.35	0.06	0.22	0.05	0.40	0.39	0.90
46 to 53	0.11	0.40	0.05	0.23	0.05	0.43	0.42	1.04
55 to 64	0.10	0.61	0.06	0.29	0.06	0.81	0.44	1.32
66 to 76	0.12	0.78	0.09	0.34	0.10	1.12	0.50	1.64
79 to 91	0.13	1.00	0.11	0.47	0.20	3.42	0.55	4.94
95 to 106	0.33	1.14	0.14	0.64	0.17	4.29	0.89	5.90

Table S3. F_{inf} estimates (associated uncertainties, ± SE) and ratios of mean indoor and outdoor concentrations (C_{in}/C_{out}) (associated uncertainties, ± SE) for selected representative tests and particle sizes

TEST ID	*Finf* (± SE)			Avg. I-O Ratio (± SE)		
	9-11 nm	38-44 nm	79-91 nm	9-11 nm	38-44 nm	79-91 nm
LWOn1	0.48(0.03)	0.76(0.04)	0.82(0.04)	0.52(0.04)	0.75(0.02)	0.83(0.02)
LWOn2	0.35(0.02)	0.69(0.04)	0.78(0.04)	0.52(0.03)	0.71(0.02)	0.77(0.02)
LWOn6	0.57(0.03)	0.77(0.04)	0.81(0.04)	0.52(0.03)	0.72(0.04)	0.75(0.04)
SWOn1	0.14(0.01)	0.41(0.03)	0.55(0.05)	0.16(0.01)	0.38(0.01)	0.51(0.01)
SWOn2	0.12(0.01)	0.45(0.03)	0.59(0.06)	0.13(0.01)	0.44(0.01)	0.58(0.01)
SWOn6	0.13(0.01)	0.44(0.01)	0.58(0.02)	0.15(0.01)	0.42(0.01)	0.56(0.01)
CWOff1	0.06(0.01)	0.32(0.07)	0.41(0.15)	0.07(0.004)	0.33(0.01)	0.43(0.01)
CWOff2	0.08(0.01)	0.40(0.05)	0.55(0.08)	0.07(0.004)	0.30(0.01)	0.54(0.02)
CWOff4	0.03(0.002)	0.26(0.02)	0.41(0.03)	0.03(0.001)	0.29(0.01)	0.43(0.01)
SWOff1	0.27(0.03)	0.62(0.07)	0.67(0.09)	0.26(0.01)	0.60(0.01)	0.67(0.02)
SWOff2	0.26(0.03)	0.60(0.09)	0.74(0.11)	0.26(0.01)	0.58(0.02)	0.73(0.01)
SWOff4	0.37(0.04)	0.78(0.10)	0.85(0.11)	0.44(0.03)	0.74(0.05)	0.81(0.01)

Table S4. Average F_{inf} estimates vs. ratios of mean indoor and outdoor concentrations (C_{in}/C_{out})

Particle Diameter (nm)	Central Fan On						Central Fan off					
	Small Window Opening (SW)			Large Window Opening (LW)			Small Window Opening (SW)			Closed Windows (CW)		
	F_{inf}	I/O ratio	% Diff.	F_{inf}	I/O ratio	% Diff.	F_{inf}	I/O ratio	% Diff.	F_{inf}	I/O ratio	% Diff.
4.4 to 5.1				0.26	0.36	**16.1**						
5.3 to 6.2				0.33	0.42	**12.0**	0.25	0.22	**6.4**			
6.4 to 7.4	0.07	0.11	**22.2**	0.38	0.46	**9.5**	0.24	0.28	**7.7**	0.01	0.02	**33.3**
7.6 to 8.8	0.12	0.14	**7.7**	0.40	0.50	**11.1**	0.26	0.30	**7.1**	0.03	0.04	**14.3**
9 to 11	0.14	0.16	**6.7**	0.44	0.52	**8.3**	0.29	0.32	**4.9**	0.05	0.07	**16.7**
11 to 13	0.17	0.18	**2.9**	0.46	0.55	**8.9**	0.33	0.36	**4.3**	0.07	0.08	**6.7**
13 to 15	0.20	0.21	**2.4**	0.49	0.58	**8.4**	0.39	0.42	**3.7**	0.09	0.11	**10.0**
16 to 18	0.24	0.25	**2.0**	0.54	0.61	**6.1**	0.42	0.45	**3.4**	0.12	0.14	**7.7**
19 to 22	0.28	0.29	**1.8**	0.58	0.63	**4.1**	0.47	0.50	**3.1**	0.15	0.18	**9.1**
22 to 26	0.33	0.33	**0.0**	0.63	0.66	**2.3**	0.52	0.55	**2.8**	0.18	0.21	**7.7**
27 to 31	0.37	0.37	**0.0**	0.67	0.68	**0.7**	0.56	0.58	**1.8**	0.22	0.26	**8.3**
32 to 37	0.41	0.40	**1.2**	0.71	0.70	**0.7**	0.59	0.61	**1.7**	0.26	0.30	**7.1**

38 to 44	0.45	0.44	**1.1**	0.74	0.72	**1.4**	0.64	0.63	**0.8**	0.30	0.36	**9.1**
46 to 53	0.49	0.47	**2.1**	0.76	0.73	**2.0**	0.67	0.66	**0.8**	0.36	0.41	**6.5**
55 to 64	0.52	0.50	**2.0**	0.77	0.74	**2.0**	0.69	0.68	**0.7**	0.40	0.45	**5.9**
66 to 76	0.56	0.53	**2.8**	0.79	0.76	**1.9**	0.71	0.70	**0.7**	0.43	0.49	**6.5**
79 to 91	0.58	0.56	**1.8**	0.80	0.77	**1.9**	0.72	0.70	**1.4**	0.46	0.52	**6.1**
95 to 106	0.60	0.58	**1.7**	0.81	0.78	**1.9**	0.72	0.71	**0.7**	0.48	0.56	**7.7**

Table S5. A summary of experimental studies on UFP infiltration factor and I/O ratio

Reference Source	Particle Size Range	Locations	F_{inf}	I/O ratio	Detailed Results
Kearney et al. (2011)	20 nm - 1μm, number integrated	92 homes in Windsor, ON, Canada	0 – 0.79	0.03-0.87	Lower F_{inf} values (0.04-0.35) during winter than summer
Mullen et al. (2011)	6 nm – 100 nm, number integrated	4 high-rise apartment buildings in Beijing, China		0.39-1.16	0.27-0.39 with windows closed & 0.65-0.78 with windows open
Bhangar et al. (2011)	6 nm – 100 nm, number integrated	7 single-family houses in northern California	0.11 – 0.47		2-4 times higher with ventilation system/filtration turned off
McAuley et al. (2010)	6 nm - 165 nm, size resolved	5 homes in Buffalo, NY		0.12-0.52	Highest value for 70–165 nm and lowest value for 20 nm
Rim et al. (2010)	4 nm – 100 nm, size-resolved	a test house in the suburban Washington D.C. area	0.03- 0.47	0.03-0.45	Lower I/O ratios (0.03-0.20) for closed windows
Hahn et al. (2009)	20 nm to 1μm, integrated	A near highway urban residence building in Brooklyn, NY,		0.10-0.32	Lower values (0.10-0.25) for the first floor compared to the values (0.22 – 0.32) for the second floor
Zhu et al. (2005)	6 nm – 220 nm, size resolved	4 two-bedroom apartments within 60m from a major freeway in Los Angeles, CA		0.1- 1.0	The highest values (0.6–0.9) for 70–100 nm and the lowest values (0.1–0.4) for 10–20 nm

Table S6. A summary of experimental studies on infiltration factor for $PM_{2.5}$ (Chen et al. 2011)

Reference	Location	Particle Type	F_{in} (mean)	Conditions
Meng et al. (2009)	Three Cities, USA	$PM_{2.5}$	0.63	32 homes; 0 smoking; Central AC;
			0.72	32 homes; 0 smoking; No Central AC;
Hoek et al. (2008)	Helsinki, Finland	$PM_{2.5}$	0.51	37 homes; 0 smoking; 5 Mechanical ventilation;
		PM10	0.17	
	Athens, Greece	$PM_{2.5}$	0.3	35 homes; 6 smoking; 13 Mechanical ventilation;
		PM10	0.28	
	Amsterdam, Netherlands	$PM_{2.5}$	0.38	50 homes; 2 smoking; 1 Mechanical ventilation;
		PM10	0.41	
	Birmingham, UK	$PM_{2.5}$	0.37	30 homes; 4 smoking; 1 Mechanical ventilation;
		PM10	0.27	
Meng et al. (2007)	Houston, USA	$PM_{2.5}$, primary combustion	0.51	81 homes; No smoking;
		$PM_{2.5}$, secondary formation	0.48	
	L.A. County, USA	$PM_{2.5}$, primary combustion	0.66	104 homes; No smoking;
		$PM_{2.5}$, secondary formation	0.82	
	Elizabeth, USA	$PM_{2.5}$, primary combustion	0.65	78 homes; No smoking;
		$PM_{2.5}$, secondary formation	0.63	
Sarnat et al. (2006)	L.A. USA	$PM_{2.5}$	0.48	17 homes; No smoking;
Bennet and Koutrakis (2006)	Boston .USA	0.02-0.03μm	0.49	9 homes; Size-dependent;
		0.2-0.3μm	0.76	
		4-6μm	0.32	
Reff et al. (2005)	Three cities. USA	$PM_{2.5}$	0.51	172 homes;
Wallace and Williams (2005)	North Carolina. USA	$PM_{2.5}$	0.55	37 homes; Have indoor sources;
Haonninen et al. (2004)	Athens. Greece	$PM_{2.5}$	0.7	Residences;
	Basle. Switzerland		0.63	
	Helsinki. Finland		0.59	
	Prague. Czech		0.61	
Williams et al. (2003)	North Carolina. USA	$PM_{2.5}$	0.45	37 homes; Have occupant; No smoking;
Wallace et al. (2003)	Seven cities. USA	$PM_{2.5}$	0.48	294 homes; Occupant;
Allen et al. (2003)	Seattle, USA	PM (using light scattering)	0.69	44 homes; Open windows;
			0.58	44 homes; Closed windows;

Landis et al. (2001)	Baltimore. USA	$PM_{2.5}$	0.35	1 home; No occupant;
Long et al. (2001)	Boston, USA	$PM_{2.5}$	0.7	9 homes; No smoking; Naturally ventilation;
Lachenmyer and Hidy (2000)	Birmingham. USA	$PM_{2.5}$	0.66	10 homes; No smoking;
Lee et al. (1997)	Chongju. Korea	$PM_{2.5}$	0.62	1 lecture room; No occupant;
Ozkaynak et al. (1993)	Riverside. USA	$PM_{2.5}$	0.7	178 homes; Daytime;
Ozkaynak et al. (1993)	Riverside. USA	$PM_{2.5}$	0.56	178 homes; Overnight;